#### STOCHASTICS AND PROBABILITY IN ENGINEERING MECHANICS



# Rapid uncertainty quantification for non-linear and stochastic wind excited structures: a metamodeling approach

Wei-Chu Chuang · Seymour M. J. Spence

Received: 6 August 2018/Accepted: 13 February 2019/Published online: 28 February 2019 © Springer Nature B.V. 2019

**Abstract** The application of performance-based design (PBD) requires the modeling of the dynamic response of the system beyond the elastic limit. If probabilistic PBD is considered, this implies the need to propagate uncertainties through non-linear dynamic systems. This paper investigates the possibility of using advanced metamodeling techniques in order to define a computationally tractable approach for propagating uncertainty through a class of multi-degree-offreedom non-linear dynamic systems subject to multivariate stochastic wind excitation. To this end, a scheme is introduced that is based on combining model order reduction with a recently introduced metamodeling approach that has been seen to be particularly effective in describing the dynamic response of uncertain non-linear systems of low dimensions. A case study consisting in a 40-story moment resisting frame subject to multivariate stochastic wind excitation and an array of non-linear viscous dampers is presented to illustrate the potential of the scheme.

 $\begin{tabular}{ll} Keywords & Metamodeling \cdot Reduced order \\ modeling \cdot Uncertain dynamic systems \cdot Monte Carlo \\ simulation \cdot Wind engineering \cdot Multi-degree-of-freedom systems \\ \end{tabular}$ 

W.-C. Chuang · S. M. J. Spence (⊠) Department of Civil and Environmental Engineering, University of Michigan, Ann Arbor, MI 48109, USA e-mail: smjs@umich.edu

#### 1 Introduction

In the design of building systems against natural hazards, performance-based design (PBD) has grown in popularity over the past years owing to the advantages that an approach of this kind can offer in terms of both the reliability and cost [1-4]. In order to apply such an approach, particular attention must be devoted to understanding and modeling the behavior of the system over a full range of hazard levels, i.e. from serviceability to possible collapse. From a computational standpoint, it is the estimation of the extreme responses that often becomes computationally challenging, as non-linear dynamic systems generally have to be considered [5]. This computational challenge becomes particularly noteworthy in the case of modern probabilisite PBD where uncertainty must be propagated through the system for estimating performance [2, 4, 6–10].

An approach for overcoming these difficulties, which has recently gained significant interest, is that offered by metamodeling. The basic idea in this approach is to define a metamodel (also known as a surrogate model) of the original system that is computationally efficient to evaluate. This allows any uncertainty to be easily propagated through the system using methods such as Monte Carlo simulation. In general, to calibrate the metamodel, a training process must be carried out that entails running the original computationally burdensome model in a limited number of carefully chosen points. Recently,



researchers have been developing metamodeling approaches for describing the stochastic response of uncertain non-linear systems driven by stochastic excitation [11, 12]. Of particular interest to this work is a recently proposed numerical approach based on combining polynomial chaos (PC) expansions and non-linear autoregressive with exogenous input (NARX) models [11, 12]. In this approach, NARX models are used to capture the dynamic behavior of the system, while polynomial chaos expansions (PCEs) are adopted to treat the uncertainties in the system properties. The resulting metamodel has been seen to be effective in accurately reproducing the response of several earthquake engineering applications involving stochastic excitation [11, 12]. Current limitations of the approach lie in difficulties associated with identifying appropriate NARX models in the case of multidegree-of-freedom systems [13], and in its singleinput single-output structure. This last is particular limiting in the case of wind excited structures due to the inherently multivariate nature of wind loads.

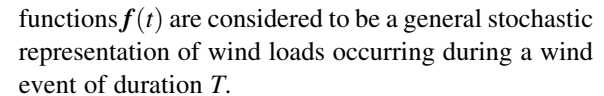
To overcome these limitations, in this work, the possibility of combining this metamodeling approach with a modal-based model reduction scheme will be investigated with the aim of defining an efficient framework for the propagation of uncertainty through a class of non-linear and uncertain multi-degree-of-freedom systems subject to multivariate stochastic wind excitation.

## 2 Problem definition

The general class of non-linear systems of interest to this work can be cast, for an *N*-degree-of-freedom system, in the following form:

$$M\ddot{u}(t) + C\dot{u}(t) + Ku(t) + f_{nl}(t; u, \dot{u}) = f(t; \bar{v})$$
 (1)

where:  $\dot{\boldsymbol{u}}(t)$ ,  $\ddot{\boldsymbol{u}}(t)$  and  $\boldsymbol{u}(t)$  are the  $N\times 1$  velocity, acceleration and displacement response vectors;  $\boldsymbol{M}$ ,  $\boldsymbol{C}$  and  $\boldsymbol{K}$  are the  $N\times N$  mass, damping and linear stiffness matrices of the system;  $\boldsymbol{f}(t)$  is a  $N\times 1$  external vector of multivariate stochastic wind excitation;  $\bar{\boldsymbol{v}}$  is the mean wind speed to which  $\boldsymbol{f}(t)$  is calibrated; and  $\boldsymbol{f}_{nl}(t)$  is a  $N\times 1$  vector of non-linear restoring forces that depend on the system response. In the following, it will be assumed that the matrices  $\boldsymbol{M}$ ,  $\boldsymbol{C}$  and  $\boldsymbol{K}$  are constant in time, while the forcing



To propagate uncertainty through Eq. (1) in the presence of system uncertainties, e.g. uncertainties in the damping and stiffness, as well as general stochastic loads, simulation methods are generally required. This is especially true if performance of a system is to be characterized within modern performance-based wind engineering frameworks, where performance is assessed in terms of correlated sample sets of peak responses occurring in [0, T] [2, 4, 6–10]. This work is focused on developing a metamodeling approach for efficiently propagating uncertainty through the nonlinear system of Eq. (1) within a stochastic simulation environment.

# 3 The proposed approach

#### 3.1 Reduced order model

Because of the structure of Eq. (1), i.e. existence of a time independent elastic stiffness K, a straightforward approach to define a reduced order model for the nonlinear  $N \times N$  system of Eq. (1) is to carry out modal analysis on the left-hand side of the following system [14–20]:

$$M\ddot{\boldsymbol{u}}(t) + C\dot{\boldsymbol{u}}(t) + K\boldsymbol{u}(t) = \boldsymbol{f}(t; \bar{\boldsymbol{v}}) - \boldsymbol{f}_{nl}(t; \boldsymbol{u}, \dot{\boldsymbol{u}})$$
 (2)

According to this approach, the dynamic response of the system can be estimated through the following set of non-linear equations [14–17]:

$$M_{m}\ddot{y}_{m}(t) + 2M_{m}\omega_{m}\zeta_{m}\dot{y}_{m}(t) + M_{m}\omega_{m}^{2}y_{m}(t)$$

$$= \Phi_{m}^{T}[f(t; \bar{v}) - f_{nl}(t; \boldsymbol{u}, \dot{\boldsymbol{u}})]$$

$$= Q_{m}(t; \bar{v}) + \Phi_{m}^{T}f_{nl}(t; \boldsymbol{u}, \dot{\boldsymbol{u}}),$$

$$m = 1, \dots, N_{m} < N$$
(3)

where:  $\ddot{y}_m$ ,  $\dot{y}_m$  and  $y_m$  are the generalized responses of the system;  $M_m$ ,  $\omega_m$ ,  $\zeta_m$  and  $\Phi_m$  are respectively the mth generalized mass, natural circular frequency, damping ratio and mode shape associated with the left-hand side of Eq. (2); while  $Q_m(t)$  is the generalized forcing function. In general, the damping ratio,  $\zeta_m$ , can be directly assigned, while  $M_m$  and  $\omega_m$  can be estimated as:



$$M_{m} = \Phi_{m}^{T} M \Phi_{m}$$

$$\omega_{m}^{2} = \frac{1}{M_{m}} \Phi_{m}^{T} K \Phi_{m}$$
(4)

where the mode shapes are estimated from solving a standard eigenvalue/eigenvector problem in terms of M and K. Once the generalized responses are known, the responses in physical coordinates can be estimated through the transformation:

$$\mathbf{u}(t) = \mathbf{\Phi}_{N_m} \mathbf{y}_{N_m}(t) 
\dot{\mathbf{u}}(t) = \mathbf{\Phi}_{N_m} \dot{\mathbf{y}}_{N_m}(t) 
\ddot{\mathbf{u}}(t) = \mathbf{\Phi}_{N_m} \ddot{\mathbf{y}}_{N_m}(t)$$
(5)

where  $\Phi_{N_m}$  is the modal matrix collecting the first  $N_m \leq N$  modes while  $\mathbf{y}_{N_m}$ ,  $\dot{\mathbf{y}}_{N_m}$  and  $\ddot{\mathbf{y}}_{N_m}$  are the generalized response vectors collecting the responses of the first  $N_m$  generalized coordinates.

The advantage of the non-linear system of Eq. (3) is that, in general, only the first few modes are necessary to accurately predict the response of the system, i.e.  $N_m$  can be taken such that  $N_m \ll N$ . This has been illustrated in a number of applications involving structures subject to stochastic seismic excitations and governed by non-linear equations of the type shown in Eq. (2) [14–17]. In practice, through the reduction of this section, the state of the non-linear system is governed by the reduced set of variables,  $\{y_{N_m}(t), \dot{y}_{N_m}(t), \ddot{y}_{N_m}(t)\}$  as opposed to  $\{u(t), \dot{u}(t), \ddot{u}(t), \ddot{u}(t)\}$ .

Notwithstanding the order reduction, as outlined in [17], the system of Eq. (3) still requires to be solved simultaneously through an appropriate step-by-step integration scheme, such as the Newmark constant acceleration method [17] or fast non-linear analysis [21]. In cases where uncertainty is to be propagated through the system using approaches such as Monte Carlo simulation, this can fast become computationally cumbersome. To overcome this, the possibility of using appropriate metamodeling schemes for rapidly propagating uncertainty through the reduced system of Eq. (3) will be investigated.

# 3.1.1 Uncertainty modeling

The reduced system of Eq. (3) provides a convenient setting for modeling uncertainties in the system parameters, e.g. damping and stiffness. Indeed, there are a number of studies that have been carried out that

characterize the uncertainty in the modal quantities, i.e.  $\omega_m$  and  $\zeta_m$ , of wind excited systems [2, 22–24]. Therefore, once the reduced system is defined, uncertainty can be modeled directly at the level of the natural frequencies and damping ratios of the reduced system through assigning appropriate probability distributions. In alternative, a direct approach can also be taken, in which the uncertainties are modeled at the level of **K** and **M**. In this case, the modal matrix,  $\Phi_{N_m}$ , becomes uncertain and requires evaluation for each realization of the uncertainties affecting K and M. However, because this only requires the evaluation of a standard eigenvalue/eigenvector problem, it does not represent a significant computational challenge. Together with these uncertainties, in general, uncertainties characterizing the intensity of the stochastic excitation, e.g. the wind speed  $\bar{v}$ , as well as the properties of the non-linear components generating the restoring forces  $f_{nl}$ , will require modeling. These additional sources of system uncertainty can be incorporated, without difficulty, in the reduced order model directly at the level of the non-linear components and stochastic wind load model. In the following, all uncertainties associated with the elastic system parameters, external excitation model and non-linear components will be collected in the uncertain vector  $\boldsymbol{X}$ .

## 3.2 A metamodel-based solution scheme

Recently, a metamodeling approach has been proposed for efficiently simulating the response of uncertain non-linear systems excited by stochastic loads [11, 12]. The approach has been seen to be particularly well suited to single-input single-output low dimensional non-linear systems subject to stochastic excitation, e.g. earthquake loads [12]. With this mind, it is interesting to observe that, independently of whether the original stochastic excitation is multivariate or not, each generalized coordinate of the reduced system of Eq. (3) can be treated as a single-input  $(Q_m)$  single-output  $(y_m, \dot{y}_m)$ or  $\ddot{y}_m$  depending on the variable of interest) system. Within this context, consider representing the input/ output relationship of the mth generalized coordinate through the following NARX model (where the dependency on the mth coordinate is not explicitly shown for clarity of presentation) [25]:



$$y(t_{j}) = G(\mathbf{z}(t_{j})) + \epsilon(t_{j})$$
  
=  $G(Q(t_{j}), ..., Q(t_{j-n_{Q}}), y(t_{j-1}), ..., y(t_{j-n_{y}})) + \epsilon_{t}$   
(6

where:  $y(t_j)$ ,  $Q(t_j)$  and  $\epsilon(t_j)$  are the system output, input and noise sequences at discrete time step  $t_j$ , respectively;  $n_y$  and  $n_Q$  are the maximum lags for the system input and output;  $G(\cdot)$  is the underlying nonlinear approximator to be identified;  $\mathbf{z}(t_j)$  is the regression vector collecting the system outputs and inputs at time step  $t_j$ ; while  $\epsilon_t$  is a normal random variable with zero mean and standard deviation  $\sigma_\epsilon(t_j)$  (i.e.  $\epsilon_t \sim N(0, \sigma_\epsilon^2(t_j))$ ) representing the residual error of the NARX model. Equation (6) above can then be expressed in a commonly used linear-in-the-parameters form:

$$y(t_j) = \sum_{i=1}^{n_g} \vartheta_i \, g_i(\mathbf{z}(t_j)) + \epsilon_t \tag{7}$$

in which  $n_g$  is the number of potential model terms  $g_i(\mathbf{z}(t_j))$  that are functions of the regression vector,  $\mathbf{z}(t_j)$ , while  $\vartheta_i$  are the corresponding parameters of the NARX model. In general, the identification of the NARX model consists in firstly selecting the correct model structure (i.e. selecting the NARX terms  $g_i(\mathbf{z}(t))$  of the model), and secondly estimating the model parameters,  $\vartheta_i$ , from the system inputs and outputs. To this end, several approaches have been proposed for identifying the simplest model that can appropriately represent the underlying dynamics of non-linear systems [25–27].

Once calibrated, the NARX model of Eq. (7) is capable of capturing the time evolution of the system in the time interval [0, T], i.e. given a realization of the generalized force,  $Q(t_i)$  with  $t_i = 0, \Delta t, 2\Delta t, ..., N_T \Delta t$ with  $N_T$  the total number of discrete time steps of duration  $\Delta t$  in [0, T], Eq. (7) can be used to estimate the output discrete time series  $y(t_i)$ . In particular, models of this type can be constructed not only for the displacement responses, but also for the velocities,  $\dot{y}(t_i)$ , and accelerations,  $\ddot{y}(t_i)$ . What the NARX models cannot capture are the effects of uncertainties in the system parameters, i.e. the uncertainties collected in X and discussed in Sect. 3.1.1. A recently proposed approach for capturing this type of system uncertainty, and that will be followed here, is to consider the parameters,  $\vartheta_i$ , of the NARX model as deterministic functions of the system uncertainties. In particular, this functional relationship can be estimated through a truncated PCE:

$$\vartheta_i(\mathbf{X}) = \sum_{l=1}^{n_{\psi}} \vartheta_{i,l} \psi_l(\mathbf{X}) + \epsilon_i \tag{8}$$

where X is the vector collecting all the system uncertainties,  $\epsilon_i$  is the truncation error,  $\psi_l(X)$  for  $l=1,\ldots,n_\psi$  are multivariate orthonormal polynomials associated with X, while  $\vartheta_{i,l}$  for  $i=1,\ldots,n_g$  and  $l=1,\ldots,n_\psi$  are the associated deterministic polynomial chaos coefficients.

By combining the truncated PCE representation of the coefficients with the NARX model of Eq. (7), the following PC-NARX metamodel of the input/output relationship of the generalized coordinates of the reduced model of Sect. 3.1 is obtained:

$$y(t_j, \mathbf{X}) = \sum_{i=1}^{n_g} \sum_{l=1}^{n_{\psi}} \vartheta_{i,l} \psi_l(\mathbf{X}) \, g_i(\mathbf{z}(t_j)) + \epsilon(t_j, \mathbf{X})$$
(9)

with  $\epsilon(t_i, X)$  designating the total error due to the truncation of the PCE and the noise of the NARX model. To calibrate Eq. (9), it is first necessary to identify a full NARX model, i.e. an initial set of NARX terms  $g_i(\mathbf{z}(t_i))$  and maximum output,  $n_v$ , and input,  $n_O$ , lags from which the model structure can be selected. In general, this can be achieved based on the known mechanical properties of the structural system to be approximated (e.g. type of non-linearity). From the full NARX model, the model structure, i.e. most important NARX terms, can be identified through the scheme that will be outlined in the next section. The parameters,  $\vartheta_i$ , of the identified model structure can then be represented through the PCE of Eq. (8) where the number of terms,  $n_{\psi}$ , to consider in the expansion can be automatically identified from the input/output data generated for identifying the model structure and the least angle regression (LARS) based scheme outlined in [12, 28].

## 3.2.1 Non-intrusive metamodel calibration

Given an appropriate full NARX model, a nonintrusive approach for identifying the model structure and associated parameters has been recently proposed in [12]. In particular, this approach is based on selecting the model structure through a LARS algorithm, while estimating the corresponding parameters through the optimization of the one-step-ahead



prediction error (PE). This approach has been seen to provide good accuracy in reproducing the response of non-linear dynamic systems subject to short duration stochastic excitation, e.g. seismic loads. However, wind excitation has a much longer duration of sustained loading which can easily lead to a serious error accumulation problem, i.e. small prediction errors accumulating to larger ones due to the model output feedback. In extreme situations, the model can become unstable (i.e. predictions that tend to infinity), even if the model still possesses very good one-step ahead prediction performance.

In this work, the approach suggested in [12] for refining the selection of the parameters of the NARX model will be investigated as a means to avoid the error accumulation problem encountered in using the PE-based LARS algorithm for calibrating the PC-NARX model of Eq. (9). To this end, consider an experimental design consisting in K realizations of the generalized forces,  $Q_k(t_j)$  for k = 1, ..., K, and realizations of the system uncertainties,  $x_k$  for k = 1, ..., K. By following the PE-based LARS algorithm outlined in [12], an appropriate model structure can be identified. This process provides an initial estimate of the NARX parameters for each of the K experiments through a PE criterion. Based on these values, the response to  $Q_k(t_j)$  can be simulated as:

$$\hat{y}_k(t_j; \mathbf{x}_k) = \sum_{i=1}^{n_g} \vartheta_{ki}(\mathbf{x}_k) \, g_i(\hat{\mathbf{z}}_k(t_j)) \tag{10}$$

where  $\hat{z}_k(t_j) = (Q_k(t_j), \ldots, Q_k(t_{j-n_Q}), \ \hat{y}_s(t_{j-1}), \ldots, \hat{y}_s(t_{j-n_y}))^T$ , while  $\vartheta_{ki}$  are the calibrated parameters of the NARX model for the kth experiment.

The difference between the simulated response,  $\hat{y}_k(t)$ , and the actual response,  $y_k(t)$ , in [0, T], can now be minimized in terms of the vector of NARX model parameters,  $\hat{\boldsymbol{\vartheta}}_k = \left\{\vartheta_{k1}, \ldots, \vartheta_{kn_g}\right\}^T$ , through the following simulation error criterion:

$$\hat{\boldsymbol{\vartheta}}_{k}(\boldsymbol{x}_{k}) = \underset{\hat{\boldsymbol{\vartheta}}_{k}}{\operatorname{argmin}} \left\{ \sum_{j=1}^{N_{T}} \left( y(t_{j}; \boldsymbol{x}_{k}, \hat{\boldsymbol{\vartheta}}_{k}) - \hat{y}_{k}(t_{j}; \boldsymbol{x}_{k}, \hat{\boldsymbol{\vartheta}}_{k}) \right)^{2} \right\}$$

$$(11)$$

By solving this optimization problem, refined estimates for the NARX parameters are obtained. In particular, this optimization problem can be solved by any appropriate non-linear optimization technique. In this work, the Nelder–Mead simplex algorithm [29] is

adopted. The execution time depends on how close the initial guess is to the optimal value of the NARX parameters and the number of NARX parameters, i.e. design variables, and is therefore relatively insensitive to the total duration of the excitation. In particular, the parameters obtained through the PE-based LARS algorithm outlined in [12] have been seen to provide a good starting point for solving the optimization problem of Eq. (11).

After identifying the refined NARX parameters, they can be expanded onto an appropriate PC basis, with corresponding deterministic coefficients, through the *K* realizations of input/output generated during the identification of the model structure and the LARS-based procedure outlined in [12, 28], therefore leading to a fully calibrated PC-NARX model. In particular, it should be observed that the calibration process outlined here is non-intrusive, as it only requires the input and output of the reduced coordinate.

# 3.3 Overall procedure

The overall procedure for defining the metamodel of order  $N_m$  for the system outlined in Eq. (2) subject to multivariate stochastic wind loads of duration T can be summarized as follows:

- 1. Generate a set of K realizations of the uncertain vector X, with associated realizations of the multivariate forcing functions  $f(t_j)$  of time step  $\Delta t$  and total duration T, through a space filling sampling procedure such as Latin hypercube sampling.
- 2. Identify the elastic modal properties of the non-linear system of Eq. (2) by carrying out an eigenvalue/eigenvector analysis in terms of *M* and *K* for each realization of *X*.
- 3. Use the mode shape vectors  $\Phi_{N_m}$  of order  $N_m$  to generate K realizations of the generalized stochastic forcing functions  $Q_{N_m}(t_j) = \Phi_{N_m}^T f(t_j)$ .
- 4. Solve the reduced order system of Eq. (3) through a direct integration approach for each realization of X and  $Q_{N_m}(t_j)$ , therefore generating K realizations of the reduced states  $\{y_{N_m}(t_j), \dot{y}_{N_m}(t_j), \ddot{y}_{N_m}(t_j), \ddot{y}_{N_m}(t_j)\}$ .
- 5. From the K discrete input/output sets of the  $N_m$  reduced coordinates, calibrate PC-NARX metamodels using the procedures outlined in Sect. 3.2.



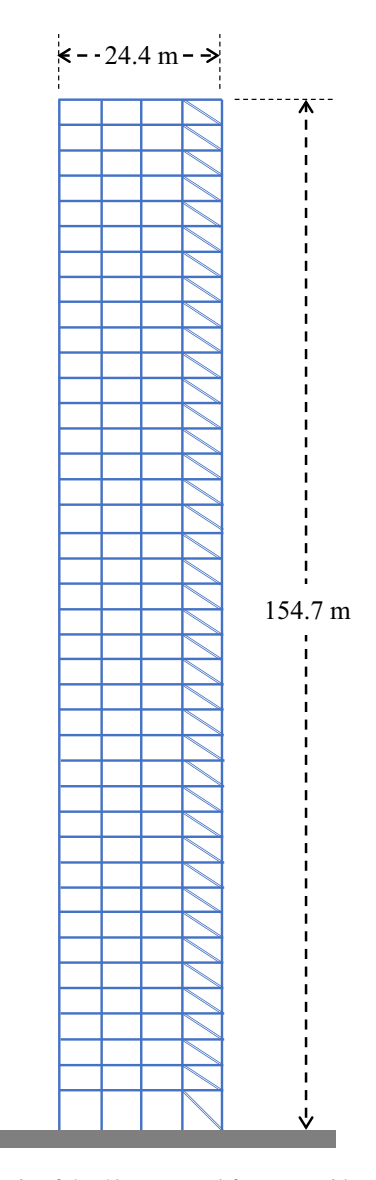
Once the metamodels of order  $N_m$  are calibrated, stochastic responses in physical coordinates can be generated by simply generating samples of X and f(t), estimating the corresponding samples  $y_{N_m}(t)$  in the reduced space, and using the transformation of Eq. (5) to estimate stochastic responses in physical coordinates. In particular, if the responses of interest are velocities and/or accelerations, PC-NARX models can be calibrated to these outputs.

# 4 Case study

In this section, a multi-degree-of-freedom building structure equipped with an array of non-linear response mitigation devices, and excited by multi-variate stochastic wind forces, is presented to illustrate the proposed metamodeling approach.

# 4.1 General description of the structure

The following results and discussion will refer to the 40-story steel frame shown in Fig. 1. The geometry of the frame is described by four 6.1 m bays and by interstory heights,  $h_i$ , of 6.1 m at ground level and 3.8 m for all other floors. The overall height of the structure, H, is 154.7 m, while the influence width W of the frame is considered to be 12.2 m. In particular, the columns were considered as square box sections while the beams were assigned standard American Institute for Steel Construction (AISC) wide flange sections. Table 1 reports the specific section sizes used in designing the structure. The mass was considered lumped at each floor with expected value calculated as the sum of the element mass and carried mass. In particular, the carried mass at each floor was taken as  $M = q_0 L/g$ , where g is the gravitational acceleration,  $q_0 = 11.96h_i$  kN/m is a uniformly distributed dead load, while  $h_i$  and L are the height and length of each floor. In this example, uncertainties were considered directly at the level of the stiffness, K, and mass, M, matrices. In particular, uncertainty in K was modeled by taking the Young's modulus of the material as a lognormal random variable with mean 210 GPa and standard deviation 15 GPa. To model the uncertainty in the mass, M was multiplied by a lognormal random variable with mean of 1 kg and standard deviation of 0.05 kg. To model uncertainty in the damping, the



 $\begin{tabular}{ll} Fig.~1 & Schematic of the 40-story steel frame considered in the case study \end{tabular}$ 

damping ratios were taken as dependent lognormal random variables with mean 0.015 and standard deviation 0.005.

As illustrated in Fig.1, response mitigation devices are diagonally mounted between each floor. In particular, these take the form of fluid viscous dampers [30] leading to the following non-linear restoring forces:



Table 1	Section	sizes of	
the steel	frame		

Level range	Wide-flange beams	Box columns		
		Interior (cm)	Exterior (cm)	
1–10	W36 × 282	56 × 56	51 × 51	
		t = 7.6	t = 6.4	
11–20	W36 × 194	51 × 51	51 × 51	
		t = 5.0	t = 5.0	
21-30	W33 × 169	$46 \times 46$	$46 \times 46$	
		t = 2.5	t = 2.5	
31–40	$W27 \times 84$	$46 \times 46$	$46 \times 46$	
		t = 1.9	t = 1.9	

t =wall thickness

$$f_{nl}(t; \dot{\boldsymbol{u}}) = \begin{cases} c_{1} \operatorname{sgn}(v_{r_{1}}) |v_{r_{1}}(\dot{u}_{1}(t))|^{\alpha} \\ \vdots \\ c_{1} \operatorname{sgn}(v_{r_{10}}) |v_{r_{10}}(\dot{u}_{10}(t), \dot{u}_{9}(t))|^{\alpha} \\ c_{2} \operatorname{sgn}(v_{r_{11}}) |v_{r_{11}}(\dot{u}_{11}(t), \dot{u}_{10}(t))|^{\alpha} \\ \vdots \\ c_{2} \operatorname{sgn}(v_{r_{20}}) |v_{r_{20}}(\dot{u}_{20}(t), \dot{u}_{19}(t))|^{\alpha} \\ c_{3} \operatorname{sgn}(v_{r_{21}}) |v_{r_{21}}(\dot{u}_{21}(t), \dot{u}_{20}(t))|^{\alpha} \\ \vdots \\ c_{3} \operatorname{sgn}(v_{r_{30}}) |v_{r_{30}}(\dot{u}_{30}(t), \dot{u}_{29}(t))|^{\alpha} \\ c_{4} \operatorname{sgn}(v_{r_{31}}) |v_{r_{31}}(\dot{u}_{31}(t), \dot{u}_{30}(t))|^{\alpha} \\ \vdots \\ c_{4} \operatorname{sgn}(v_{r_{40}}) |v_{r_{40}}(\dot{u}_{40}(t), \dot{u}_{39}(t))|^{\alpha} \end{cases}$$

$$(12)$$

where  $v_{r_j}$  is the relative velocity between the ends of the damper at floor j,  $c_1$ ,  $c_2$ ,  $c_3$  and  $c_4$  are uncertain damping coefficients with uniform distribution in [0, 100] N-s/m, while  $\alpha = 0.38$  is the damping exponent. In total, for this problem, the uncertain vector X has eight components (the mean wind speed of the next section is also taken as uncertain).

# 4.2 Stochastic wind force model

The multivariate stochastic wind loads, f(t), acting at each floor of the frame of Fig. 1 are modeled in this work through a quasi-steady model based on a spectral representation of the multivariate wind speed field acting over the height of the frame. The overall intensity of the stochastic wind loads is defined in terms of the mean hourly wind speed  $\bar{v}$  to occur at a

meteorological station of height  $H_{met}$  and roughness length  $z_{01}$ . This is related to the mean hourly wind speed over the height of the building, z, through the following transformation [23]:

$$\bar{v}_z(z_0) = 0.8065 \left(\frac{z_0}{z_{01}}\right)^{0.0706} \frac{\ln\left[\frac{z}{z_0}\right]}{\ln\left[\frac{H_{\text{met}}}{z_{01}}\right]} \bar{v}(H_{\text{met}}, z_{01}) \quad (13)$$

where  $z_0$  is the roughness length at the site of interest. In particular, in this work, the wind speed  $\bar{\nu}$  of Eq. (13) was taken as a Type II distribution with mean 30 m/s and standard deviation 3.5 m/s. A roughness length of  $z_{01}=0.05$  m and a meteorological height of  $H_{met}=10$  m were considered for  $\bar{\nu}$ . The roughness length at the site of the structure,  $z_0$ , was taken to be 0.02 m.

From Eq. (13), the *j*th component of f(t) (i.e. wind loads acting at height  $z_j$ ), can be estimated through the following quasi-steady assumption:

$$f_{j}(t) = \eta_{j}(\bar{v}_{z_{j}} + v_{z_{j}}(t))^{2} \simeq \eta_{j}(\bar{v}_{z_{j}}^{2} + 2\bar{v}_{z_{j}}v_{z_{j}}(t)),$$

$$i = 1, 2, ..., N_{f}$$
(14)

where:  $N_f = 40$  is the total number of floors;  $\eta_j$  is a coefficient given by  $\eta_j = 0.5 \rho \bar{C}_j A_j$  with  $\rho = 1.25$  kg/m<sup>3</sup> the air density,  $\bar{C}_j = 1.3$  the floor-wise quasisteady pressure coefficient, and  $A_j = h_j W$  the influence area of the *j*th component of f(t); while  $v_{z_j}(t)$  is the zero-mean fluctuating component of the multivariate stochastic wind field at height  $z_j$ . To simulate  $v_{z_j}(t)$ , the following spectral representation model can be used [31]:



$$v_{z_j}(t) = 2\sum_{m=1}^{N_f} \sum_{l=1}^{N} |H_{jm}(\omega_{ml})| \times \sqrt{\Delta\omega} \cos[\omega_{ml}(t) - \theta_{jm}(\omega_{ml}) + \phi_{ml}], \quad j = 1, 2, \dots, N_f$$
(15)

where N is the total number of components in the expansion,  $H_{jm}(\omega_{ml})$  is an element of the decomposed target cross-spectral density matrix of the fluctuating wind speeds (here taken as outlined in Appendix 1),  $\theta_{jm}(\omega_{ml})$  is the corresponding complex angle,  $\phi_{ml}$  are sequences of independent random phase angles distributed uniformly in the interval  $[0, 2\pi]$ ,  $\Delta\omega$  is the sampling frequency, while  $\omega_{ml}$  is given by:

$$\omega_{ml} = (l-1)\Delta\omega + \frac{m}{N_f}\Delta\omega, \quad l = 1, 2, \dots, N$$
 (16)

The period of the simulated wind loads is given by:

$$\hat{T} = \frac{2\pi N_f}{\Delta \omega} = \frac{2\pi N_f N}{\omega_{up}} \tag{17}$$

where  $\omega_{up}$  is the cut-off frequency. The larger the N under a specified upper cutoff frequency  $\omega_{up}$ , the longer the period of the simulated stochastic process. In particular, in the following, a storm duration of T=900 s with sampling frequency of 100 Hz will be considered. In this case, each realization of f(t) entails the generation of a total of 81,920 independent and uniformly distributed random numbers in  $[0,2\pi]$ .

# 4.3 Results

## 4.3.1 Calibration

The first three natural circular frequencies of the frame were in the range of  $\omega_1 \approx 1.5$  rad/s,  $\omega_2 \approx 4$  rad/s, and  $\omega_3 \approx 7$  rad/s. Due to how wind does not, for all intents and purposes, have energy above  $2\pi$  rad/s, the first three generalized coordinates were considered sufficient in defining the dimension of the reduced model, i.e.  $N_m = 3$ . In defining the metamodel of the displacement responses of the reduced system, i.e.  $y_m(t)$  for m = 1, 2, 3, a full NARX model was chosen as the following polynomial function:

$$g_i(t_j) = y_1^{l_1}(t_{j-n_y})Q_1^{l_2}(t_{j-n_Q})$$
(18)

with  $l_1 + l_2 \le 3$ ,  $0 \le l_1 \le 3$ ,  $0 \le l_2 \le 1$ ,  $n_y = 1, 2$  and  $n_O = 0, 1, 2$ , therefore leading to 10 candidate terms including the constant term. To identify the most appropriate NARX model, an experimental design consisting in K = 200 simulations were carried out with input random variables, i.e. X, generated by Latin hypercube sampling. From the LARS procedure of [12], four terms were selected, namely the constant term,  $Q_m(t_i)$ ,  $y_m(t_{i-1})$  and  $y_m(t_{i-2})$ . After implementing the output error procedure of Sect. 3.2.1, the mean relative error (as defined in [12]) over all 200 simulations was  $\bar{\epsilon} = 0.017$ . In representing the NARX coefficients through PCEs, adaptive expansions were considered with maximum interaction rank of 2 and truncation parameter of 1. Figure 2a shows, for one of 200 calibration points, the comparison between the reconstructed and reference displacement response (estimated through the fast non-linear analysis scheme reported in [21]) of the structure at the top floor. As can be seen, the metamodel captures the response evolution remarkably well. In particular, Fig. 2b shows the evolution of the error induced by the NARX model, while Fig. 2c reports the evolution of the overall error induced by the NARX and PC approximations. As can be seen, the overall error is not

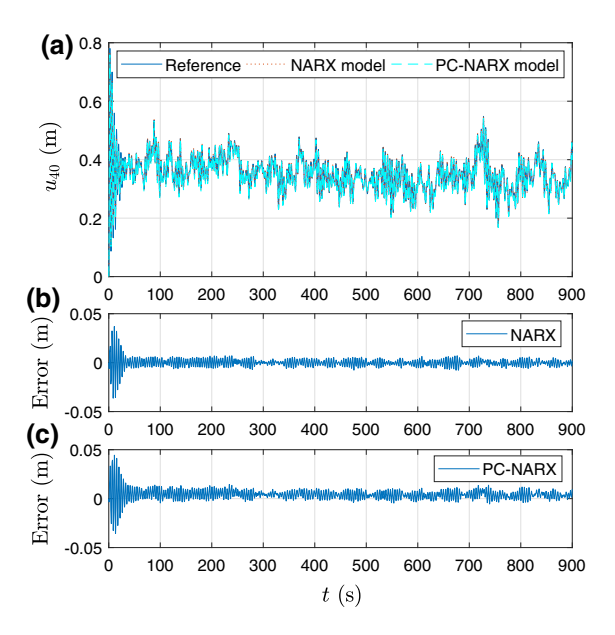


**Fig. 2** Comparison for a point of the calibration set between the reconstructed and reference top floor displacement response: **a** evolution of the response in [0, *T*]; **b** error evolution due to NARX approximation; **c** overall error evolution due to NARX and PC approximations



only small, but also stable with time, i.e. no error accumulation is seen, notwithstanding the long prediction horizon. This illustrates the effectiveness of the simulation error refinement scheme of Sect. 3.2.1.

#### 4.3.2 Simulation results

To investigate the simulation performance of the metamodel, a validation set consisting in 200 randomly generated samples of X, with associated samples of f(t), were generated. Reference solutions were estimated for each sample using once again the fast non-linear analysis scheme. The calibrated metamodel was then run for each sample and the predictive capability of the metamodel was investigated. Figure 3 shows a typical result with respect to the simulation of the coordinates of the reduced model. As can been seen, very good correspondence between the reference solutions and the reduced coordinates of the metamodel is achieved. Figure 4a reports the comparison between the reference solution and the metamodel in physical coordinates, and in particular the top floor displacement response. As can be seen, very good correspondence is achieved. Figure 4b shows the evolution of the difference between the reference and simulated responses, from which the

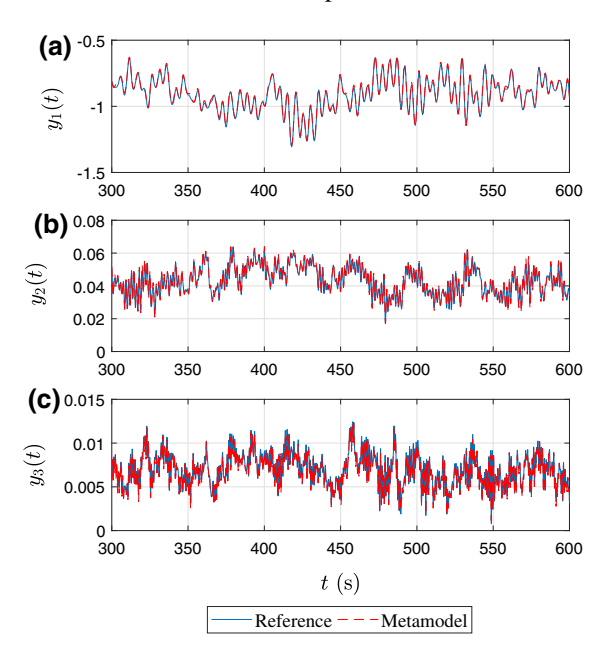


**Fig. 3** Comparison between the simulated and reference displacement responses of the reduced system for a representative sample: **a** first generalized coordinate; **b** second generalized coordinate; **c** third generalized coordinate

stability of the prediction can be seen. Similar results were seen for all simulations in the validation set. Figure 5 illustrates the typical non-linear response seen in the dampers over the duration of the event.

To illustrate the predictive capability of the metamodel over all samples, Fig. 6 reports the comparison between the 200 reference and simulated maximum absolute responses at the top floor of the structure. As can be seen, there is strong correspondence between the reference and simulated responses with a correlation coefficient of 0.97. The strong correspondence between the responses allows for the direct estimation of quantities such as the exceedance probabilities associated with the peak absolute response of the system in [0, T], as illustrated in Fig. 7.

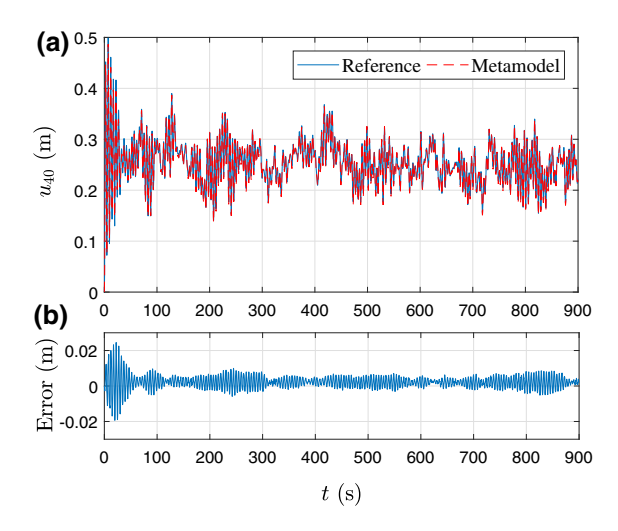


**Fig. 4** Comparison between the simulated and reference displacement responses at the top floor of the structure: **a** evolution of the response in [0, T]; **b** overall error evolution

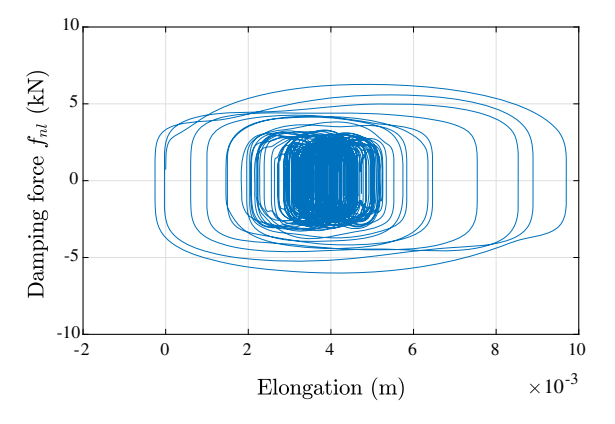
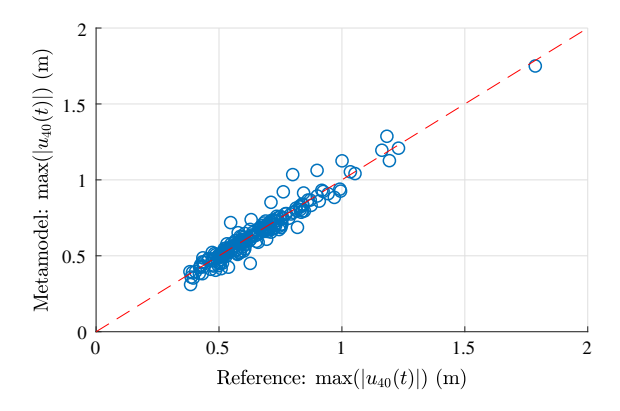


Fig. 5 Typical hysteretic response of the top floor damper





**Fig. 6** Comparison between the reference and simulated peak absolute responses in [0, T] at the top floor of the structure

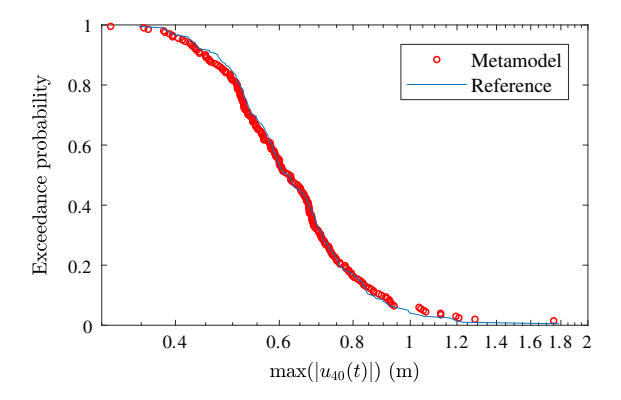
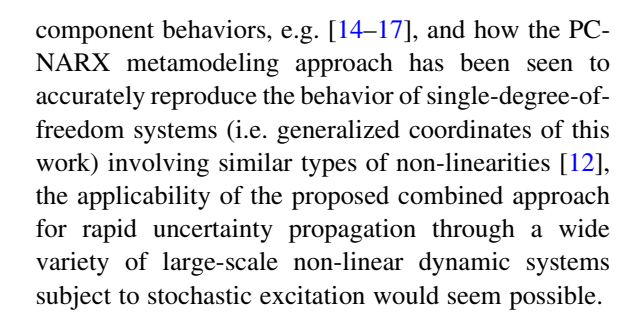


Fig. 7 Comparison between the exceedance probabilities of the top floor response estimated from the reference and simulated data

# 4.3.3 Discussion

The capability of the proposed metamodeling approach to accurately propagate uncertainty through the class of multi-degree-of-freedom non-linear systems outlined in Sect. 2 was illustrated in this section through the example structure of Fig. 1. If it is observed that, once calibrated, the generation of the response time histories through the metamodel was around two orders of magnitude faster than the fast non-linear scheme used to estimate the reference solutions, the potential of the approach becomes clear. This is especially true if it is kept in mind that the fast non-linear scheme outlined in [21] is an approach specialized for rapid resolution of the class of nonlinear systems investigated in this work. By observing how the reduction scheme of Sect. 3.1 can be applied to systems involving a wide variety of non-linear



#### 5 Conclusions

The feasibility of combining metamodeling techniques with model order reduction schemes as a means to define metamodeling approaches for the rapid propagation of uncertainty through multi-degree-of-freedom non-linear and stochastic wind excited dynamic systems was investigated in this work. To this end, a scheme was outlined based on combining a recently introduced metamodeling approach for non-linear stochastic systems with a modal-based order reduction framework. Because of the strong capability of the metamodeling approach of replicating the time evolution of a wide class of singledegree-of-freedom dynamic systems, coupled with the applicability of the reduction scheme to an equally wide class of non-linear multi-degree-of-freedom systems, the approach has the potential to be applied to a number of problems of practical interest. In particular, the possibility to calibrate the metamodel for the resolution of the reduced system in a nonintrusive mode (i.e. using only input/output) ensures the applicability to systems for which only the classic elastic modal properties are known. To demonstrate the applicability of the approach, uncertainty was propagated through a 40-story moment resisting frame equipped with an array of non-linear viscous dampers and subject to stochastic multivariate wind loads. The proposed approach was seen not only to be capable of accurately reproducing the dynamic response of the system, but also to be nearly two orders of magnitude faster than existing specialized direct integration approaches.

**Funding** This research effort was supported in part by the National Science Foundation (NSF) under Grant No. CMMI-1750339. This support is gratefully acknowledged.



#### Compliance with ethical standards

**Conflict of interest** The authors declare that they have no conflict of interest.

## **Appendix 1: Target wind spectrum**

The target power spectral density (PSD) function of the fluctuating wind velocity,  $v_{z_j}(t)$ , can be taken as [32]:

$$S_{\nu_{z_j}}(\omega) = \nu_*^2 \frac{50z_j}{\pi \bar{\nu}_{z_j}} \frac{1}{\left[1 + 50\left(\frac{\omega z_j}{2\pi \bar{\nu}_{z_j}}\right)\right]^{5/3}}$$
(19)

where  $v_*$  is the shear velocity given by:

$$v_* = \bar{v}_{10}\beta \frac{k_a}{\ln\left(\frac{10}{z_0}\right)} \tag{20}$$

where  $\bar{v}_{10}$  is the mean wind velocity at 10 m,  $\beta = 0.65$ , while  $k_a = 0.4$  is the Von Kármán's constant. The cross power spectral density can then be defined as:

$$S_{\nu_{z_j}\nu_{z_k}}(\omega) = \sqrt{S_{\nu_{z_j}}(\omega)S_{\nu_{z_k}}(\omega)}\gamma_{jk}(\omega), \quad j \neq k$$
 (21)

where  $\gamma_{jk}$  is the coherence function between  $v_{\nu_{z_j}}(t)$  and  $v_{\nu_{z_i}}(t)$  that can be modeled as [33]:

$$\gamma_{jk}(\Delta z, \omega) = \exp\left[-\frac{\omega}{2\pi} \frac{C_z \Delta z}{\frac{1}{2} (v_{z_j} + v_{z_k})}\right]$$
(22)

where  $\Delta z = |z_j - z_k|$  is the height difference, while  $C_z$  is a constant that can be set equal to 10 for design purposes [33].

#### References

- Spence SMJ, Gioffrè M (2012) Large scale reliability-based design optimization of wind excited tall buildings. Probab Eng Mech 28:206–215
- Bernardini E, Spence SMJ, Kwon DK, Kareem A (2015)
   Performance-based design of high-rise buildings for occupant comfort. J Struct Eng. https://doi.org/10.1061/ (ASCE)ST.1943-541X.0001223
- Tabbuso P, Spence SMJ, Palizzolo L, Pirrotta A, Kareem A (2016) An efficient framework for the elasto-plastic reliability assessment of uncertain wind excited systems. Struct Saf 58:69–78

- Chuang WC, Spence SMJ (2017) A performance-based design framework for the integrated collapse and non-collapse assessment of wind excited buildings. Eng Struct 150:746–758
- Gioffrè M, Gusella V (2007) Peak response of a nonlinear beam. J Eng Mech 133(9):963–969
- Ciampoli M, Petrini F, Augusti G (2011) Performancebased wind engineering: towards a general procedure. Struct Saf 33(6):367–378
- Petrini F, Ciampoli M (2012) Performance-based wind design of tall buildings. Struct Infrastruct Eng 8(10):954–966
- Caracoglia L (2014) A stochastic model for examining along-wind loading uncertainty and intervention costs due to wind-induced damage on tall buildings. Eng Struct 78:121–132
- Cui W, Caracoglia L (2015) Simulation and analysis of intervention costs due to wind-induced damage on tall buildings. Eng Struct 87:183–197
- Cui W, Caracoglia L (2017) Exploring hurricane wind speed along us atlantic coast in warming climate and effects on predictions of structural damage and intervention costs. Eng Struct 122:209–225
- Spiridonakos MD, Chatzi EN (2015) Metamodeling of dynamic nonlinear structural systems through polynomial chaos NARX models. Comput Struct 157:99–113
- Mai CV, Spiridonakos MD, Chatzi EN, Sudret B (2016) Surrogate modelling for stochastic dynamical systems by combining narx models and polynomial chaos expansions. Int J Uncertain Quantif 6:313–339
- Mai CV (2016) Polynomial chaos expansions for uncertain dynamical systems—applications in earthquake engineering. Ph.D. Thesis, ETH Zurich, Switzerland
- Eman H, Pradlwarter HJ, Schuëller GI (2000) A computational procedure for the implementation of equivalent linearization in finite element analysis. Earthq Eng Struct Dyn 29:1–17
- Pradlwarter HJ, Schuëller GI, Schenk CA (2003) A computational procedure to estimate the stochastic dynamic response of large non-linear FE-models. Comput Methods Appl Mech Eng 192:777–801
- Schenk CA, Pradlwarter HJ, Schuëller GI (2004) On the dynamic stochastic response of FE models. Probab Eng Mech 19:161–170
- Jensen HA, Catalan AA (2007) On the effects of non-linear elements in the reliability based optimal design of stochastic dynamical systems. Int J Non-Linear Mech 42:802–816
- Valdebenito MA, Schuëller GI (2011) Efficient strategies for reliability-based optimization involving non-linear, dynamical structures. Comput Struct 89:1797–1811
- Beck AT, Kougioumtzoglou IA, dos Santos KRM (2014) Optimal performance-based design of non-linear stochastic dynamical RC structures subject to stationary wind excitation. Eng Struct 78:145–153
- Mitseas IP, Kougioumtzoglou IA, Beer M (2016) An approximate stochastic dynamics approach for nonlinear structural system performance-based multi-objective optimum design. Struct Saf 60:67–76
- 21. Wilson EL (2002) Three dimensional static and dynamic analysis of structures: a physical approach with emphasis on



- earthquake engineering. Computers and Structures Inc., Berkeley
- Diniz SMC, Sadek F, Simiu E (2004) Wind speed estimation uncertainties: effects of climatological and micrometeorological parameters. Probab Eng Mech 19(4):361–371
- Diniz SMC, Simiu E (2005) Probabilistic descriptions of wind effects and wind-load factors for database-assisted design. J Struct Eng 131(3):507–516
- 24. Bashor R, Kijewski-Correa T, Kareem A (2005) On the wind-induced response of tall buildings: the effects of uncertainties in dynamic properties and human comfort thresholds. In: Proceedings of the 10<sup>th</sup> Americas conference on wind engineering
- Billings SA (2013) Nonlinear system identification: NAR-MAX methods in the time, frequency, and spatio-temporal domains. Wiley, New York
- Billings SA, Wei HL (2008) An adaptive orthogonal search algorithm for model subset selection and non-linear system identification. Int J Control 81(5):714–724
- Wei HL, Billings SA (2008) Model structure selection using an integrated forward orthogonal search algorithm assisted by squared correlation and mutual information. Int J Model Identif Control 3(4):341–356

- Blatman G, Sudret B (2011) Adaptive sparse polynomial chaos expansion based on least angle regression. J Comput Phys 230:2345–2367
- Lagarias JC, Reeds JA, Wright MH, Wright PE (1998)
   Convergence properties of the nelder-mead simplex method in low dimensions. SIAM J Optim 9(1):112–147
- Symans MD, Constantinou MC (1998) Passive fluid viscous damping systems for seismic energy dissipation. J Earthq Technol 35(4):185–206
- 31. Deodatis G (1996) Simulation of ergodic multivariate stochastic processes. J Eng Mech 122:778–787
- Kaimal JC, Wyngaard JC, Izumi Y, Coteé OR (1972)
   Spectral characteristics of surface-layer turbulence. Q J R
   Meteorol Soc 98(417):563–589
- 33. Davenport GA (1967) The dependence of wind load upon meteorological parameters. In: Proceedings of the international research seminar on wind effects on building and structures. University of Toronto Press, pp 19–82

**Publisher's Note** Springer Nature remains neutral with regard to jurisdictional claims in published maps and institutional affiliations.

